methodology, might be a promising new approach for the diagnosis of early SSc-ILD.

Objectives: To evaluate the radiotracer ^{99m}Tc-rhAnnexin V-128, which specifically targets a pathophysiologic key molecule of early apoptosis, for the detection of earliest stages of lung involvement in animal models of SSc-ILD with single photon emission computed tomography (SPECT/CT).

Methods: C57BL/6J mice were treated with a single intratracheal injection of bleomycin or saline. Animals were euthanized at days 3, 7, 14 and 21 post-injection (n=6). Lung injury was evaluated by analysis of HE and Sirius red staining. The Ashcroft score was applied for the semi-quantitative evaluation of fibrotic changes. Immunofluorescence using the TUNEL assay and double staining with specific cell markers were performed to determine apoptotic cells. Positive nuclei were quantified by manual and automatic counting with Image J analysis software. Three days after injection with bleomycin or saline, mice were injected with ^{99m}Tc-rhAnnexin V-128 (Advanced Accelerator Applications, Italy). After 1h, images were acquired using small animal SPECT/CT, followed by *ex vivo* autoradiography.

Results: In the model of bleomycin-induced lung fibrosis, inflammatory infiltrates (CD45+) occurred as early as day 3 with peak at day 7, whereas pulmonary fibrosis developed from day 7 as assessed by Sirius red staining and was most pronounced at day 21 (mean Ashcroft score=4.6, p=0.0286). Notably, the number of apoptotic cells evaluated by TUNEL staining, was highest at day 3 (mean ± SE=6.5±1.5positive cells/HPF, p=0.0436) compared with saline controls (mean ± SE=0.7±0.1, p=0.0095) and then decreased over time. To determine the type of apoptotic cells, we performed immunofluorescent co-stainings with different cell markers. Data displayed that endothelial cells (vWF+) and epithelial cells (cytokeratin+), but not inflammatory cells (CD45+) were the primary cells undergoing apoptosis in earliest inflammatory stages of ILD.

In accordance with the findings on tissue level, at day 3 post-injection, we detected *ex vivo* with autoradiography, yet not with *in vivo* SPECT/CT, an increased pulmonary uptake of ^{99m}Tc-rhAnnexin V-128 in the lungs of bleomycin-induced mice compared with saline treated controls.

Conclusions: Apoptosis of epithelial and endothelial cells preceded the development of pulmonary inflammation and fibrosis in the model of bleomycin-induced lung fibrosis. Thus, the use of ^{99m}Tc-rhAnnexin V-128 might be a promising approach for the diagnosis of earliest stages of ILD. However, sensitivity of *in vivo* imaging has to be further improved.

Disclosure of Interest: L. Guo: None declared, J. Schniering Grant/research support from: Swiss National Science Foundation (S-85605–02–01), R. Schibli: None declared, A. Blanc: None declared, D. Chicco Employee of: Advanced Accelarator Applications, S. Ye: None declared, O. Distler Grant/research support from: Actelion, Bayer, Boehringer Ingelheim, Pfizer, Sanofi;patent licensed mir-29 for the treatment of systemic sclerosis, Consultant for: 4 D Science, Actelion, Active Biotec, Bayer, BiogenIdec, BMS, Boehringer Ingelheim, ChemomAb, EpiPharm, espeRare foundation, Genentech/Roche, GSK, Inventiva, Lilly, medac, Mepha, MedImmune, Mitsubishi Tanabe Pharma, Pharmacyclics, Pfizer, Sanofi, Serodapharm, Sinoxa, Speakers bureau: AbbVie, iQone Healthcare, Mepha, M. Béhé: None declared, B. Maurer Grant/research support from: AbbVie, Protagen, EMDO, Novartis, Pfizer, Roche, Actelion. Patent licensed: mir-29 for the treatment of systemic sclerosis

DOI: 10.1136/annrheumdis-2017-eular.4945

FRI0359 THE IMPACT OF NARROWBAND ULTRAVIOLET A1 ON PROLIFERATION AND APOPTOSIS MARKERS IN ANIMAL MODEL OF SCLERODERMA

D. Karpec[1,2], R. Rudys[2], L. Leonaviciene[2], Z. Mackiewicz[2], R. Bradunaite[2], G. Kirdaite[2], R. Rugiene[1,2], A. Venalis[1,2]. [1]*Center of Rheumatology, Vilnius University;* [2]*State Research Institute Centre for Innovative Medicine, Vilnius, Lithuania*

Background: Narrowband ultraviolet A1 (UVA1) phototherapy implications for systemic sclerosis still remain the area of research.

Objectives: To define the efficacy and safety of 365±5 nm UVA1 for the dermal fibrosis treatment in bleomycin-induced mouse model of scleroderma.

Methods: DBA/2 strain mice were randomly divided to 6 groups: I – healthy animals; II – control group with bleomycin induced scleroderma, III and IV – mice with established scleroderma, treated with high and medium dose of UVA1, V and VI – healthy mice, treated with high and medium dose of UVA1. Scleroderma model was induced according to the protocol [1]. Light source emitting a narrowband UVA1 of 365±5 nm and of 21 mW/cm^2 power density was used in the study. Phototherapy was performed 3 times weekly for 5 weeks. The average cumulative doses were 1200 J/cm^2 for high and 600 J/cm^2 for medium dose treatments. Histological analysis with hematoxylin-eosin staining for dermal thickness measurement was performed. The immunohistochemical staining for p53, Ki-67 and active caspase-3 proteins was performed using specific antibodies. Statistical significance was expressed by a P value <0.05.

Results: The dermal thickness of mice treated with high and medium dose of UVA1 was significantly reduced to 272.9±113.2 and 394.0±125.9 μm, respectively, in comparison to the control group II (599.0±55.7 μm). The percentage of Ki-67 positive cells in mice with scleroderma after high- and medium-dose of UVA1 did not differ from the control group (II). The expression of p53 was significantly higher in the skin of the control group (II) compared to that of healthy mice skin (group I). After treatment of mice with scleroderma with high- and medium-dose of UVA1, the expression of p53 in the dermal layers did not differ from the control group (II) of non-treated mice. There was no change of p53 nor Ki-67 expressions between healthy (group I) and UVA1-treated healthy mice skin (groups V and VI). The statistically significant increase of active caspase-3 expression in the skin of mice with scleroderma was present after high- and medium-dose of UVA1 (groups III and IV) as compared to that of non-treated mice group (II). The expression profile of active caspase-3 did not differ between healthy (group I) and UVA1-treated healthy mice skin (groups V and VI). Results are summarized in Table 1 (Ki-67) and Figure 1 (A - active caspase-3; B - p53 immunohistochemical analysis).

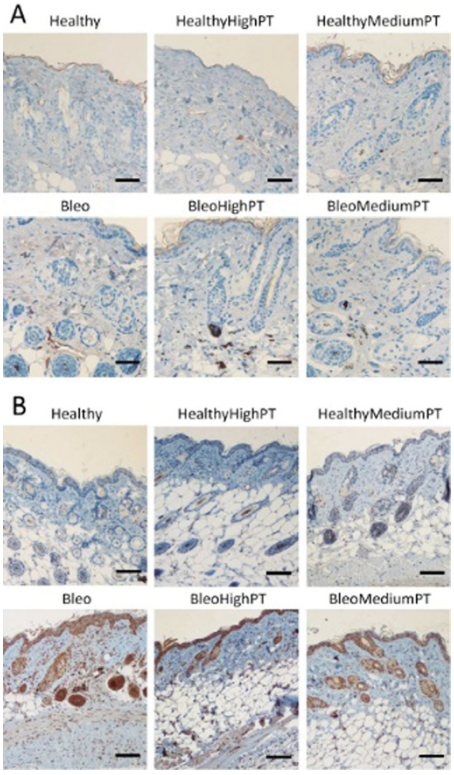

Conclusions: The cumulative doses of 1200 J/cm^2 and 600 J/cm^2 of narrowband UVA1 effectively reduced the dermal thickness, and the impact was dose-dependent. Phototherapy course did not up-regulate p53 nor Ki-67 proteins in the healthy mice and mice with scleroderma skin. UVA1 radiation caused the increase of the active caspase-3 expression in the skin of mice with scleroderma reflecting the apoptotic feature of narrowband UVA1. The results of this study indicate that 365±5 nm UVA1 phototherapy is safe and effective for the treatment of dermal fibrosis.

References:

[1] Avouac J. Mouse model of experimental dermal fibrosis: the bleomycin-induced dermal fibrosis. Methods Mol Biol 2014; 1142: 91–8.

Disclosure of Interest: None declared

DOI: 10.1136/annrheumdis-2017-eular.2869

FRI0360 ANALYSIS OF ENDOCANNABINOID SYSTEM ELEMENTS AND RELATED INFLAMMATORY MOLECULES IN PERIPHERAL BLOOD LEUKOCYTES OF PATIENTS WITH SYSTEMIC SCLEROSIS

C. Perez-Sanchez, R. Ortega-Castro, C. del Río, M.A. Aguirre, P. Ruiz-Limon, N. Barbarroja, Y. Jimenez-Gomez, I. Arias-de la Rosa, M.C. Abalos-Aguilera, E. Collantes-Estevez, E. Muñoz, C. Lopez-Pedrera. *IMIBIC/Reina Sofia University Hospital/University of Cordoba, Cordoba, Spain*

Background: The Endocannabinoid system (ECS) is a potential target for treatment of systemic sclerosis (SSc). Several cytokines/chemokines have been implicated in the induction of fibrosis in SSc, but their profile in peripheral blood

Abstract FRI0359 – Table 1

Percentage of Ki-67 positive cells	Healthy (I)	Bleo (II)	BleoHighPT (III)	BleoMediumPT (IV)	HealthyHighPT (V)	HealthyMediumPT (VI)
Average (%)	50.4	36.1	35.4	37.2	50.1	49.4
SD	2.6	3.0	3.2	2.8	2.0	1.4